Universal magnetic oscillations of DC conductivity in the incoherent regime of correlated systems

$$\hbar \frac{\mathrm{d}\mathbf{k}}{\mathrm{d}t} = -e\mathbf{v} \times \mathbf{B}$$

Rok Žitko

Jožef Stefan institute, Ljubljana, Slovenia

Faculty of Mathematics and Physics, University of Ljubljana, Slovenia

Jakša Vučičević

Scientific Computing Laboratory, Center for the Study of Complex Systems, Institute of Physics Belgrade, University of Belgrade, Serbia

Strange metals: from the Hubbard model to AdS/CFT, Institute of physics Belgrade, 25 May 2022

- Early days & recent developments in the field of quantum oscillations
- Hubbard model on square lattice in transverse magnetic field
- High-temperature quantum oscillations and the key role of velocity vertex

Fig. 1.1. First observation of oscillatory field dependence of susceptibility in bismuth (de Haas and van Alphen 1930*b*).

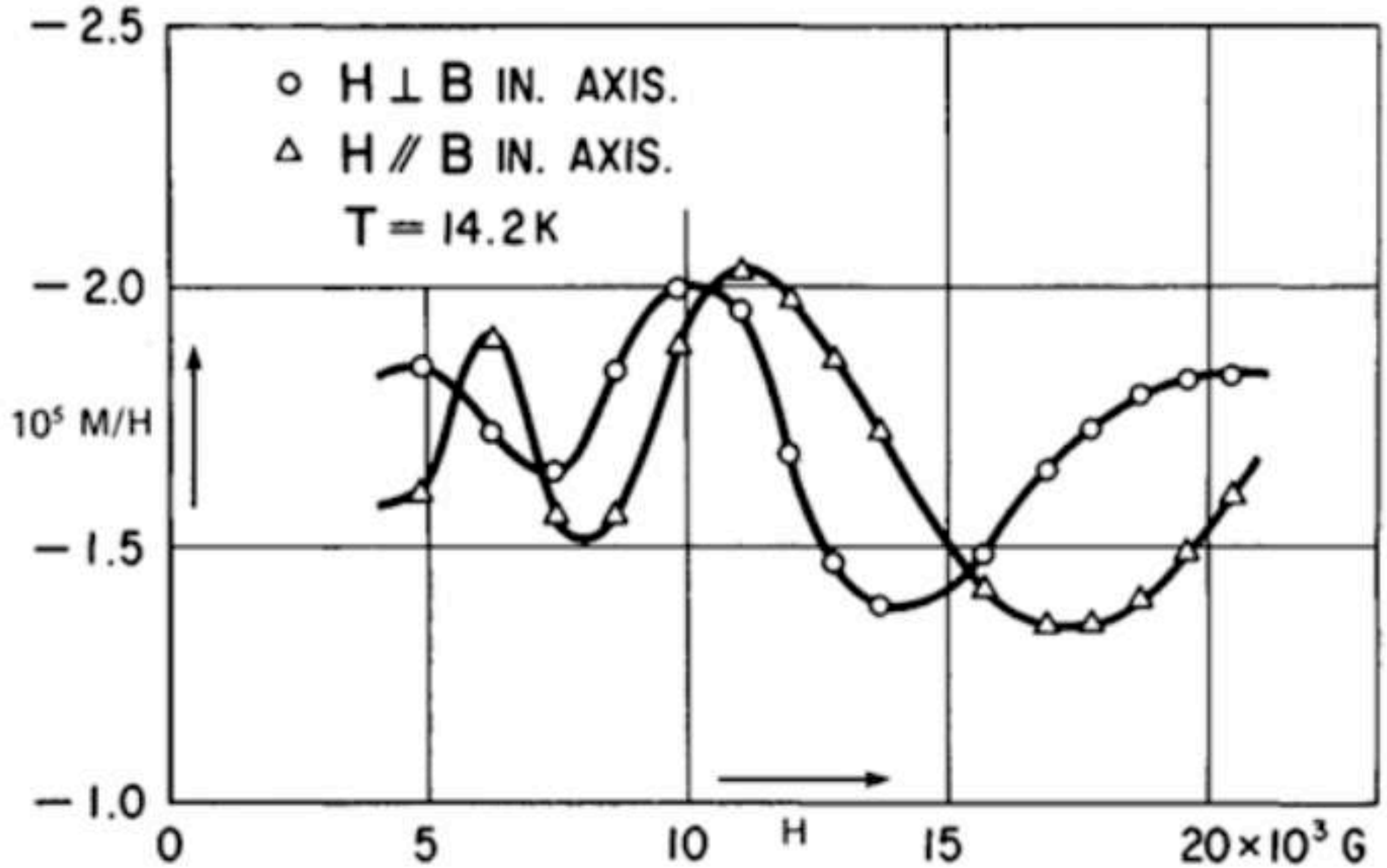

de Haas-van Alphen effect: periodic oscillations of magnetisation as a function of 1/B

Shubnikov-de Haas effect: periodic oscillations of resistivity as a function of 1/B

} magnetic/quantum oscillations

D. Schoenberg, *Magnetic Oscillations in Metals* (Cambridge University Press, Cambridge, England, 1984).

Fig. 2.1. Schematic sketches of Landau tubes for (*a*) spherical surfaces of constant energy, (*b*) ellipsoidal surfaces of constant energy (direction of long axis shown by arrow). The FS is indicated by the broken curve and only the parts of the Landau tubes inside the FS are occupied at $T = 0$ (after Chambers 1956 and Gold 1968).

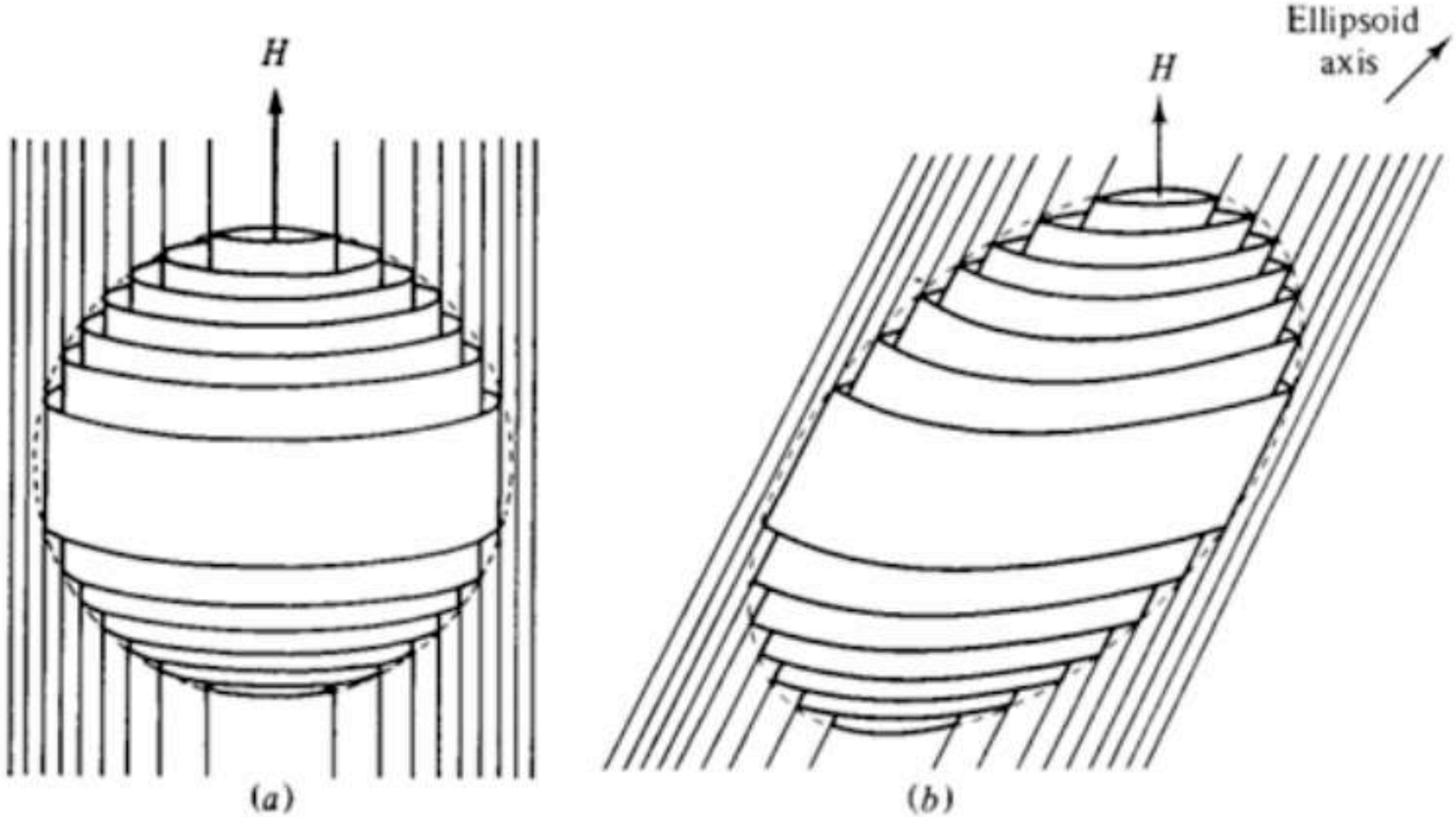

$$a(\varepsilon, k_H) = (r + \tfrac{1}{2}) 2\pi e H / \hbar c$$

A: extremal area of FS

$$\varepsilon = (r + \tfrac{1}{2}) \frac{e\hbar H}{m_0 c} + \frac{\hbar^2 k_H^2}{2m_0}$$

$$\Delta(1/H) = 2\pi e / (\hbar c A)$$

$$F = (c\hbar / 2\pi e) A$$

Passage of Landau tubes across the Fermi surface modulates the DOS (and all other quantities...)

D. Schoenberg, *Magnetic Oscillations in Metals* (Cambridge University Press, Cambridge, England, 1984).

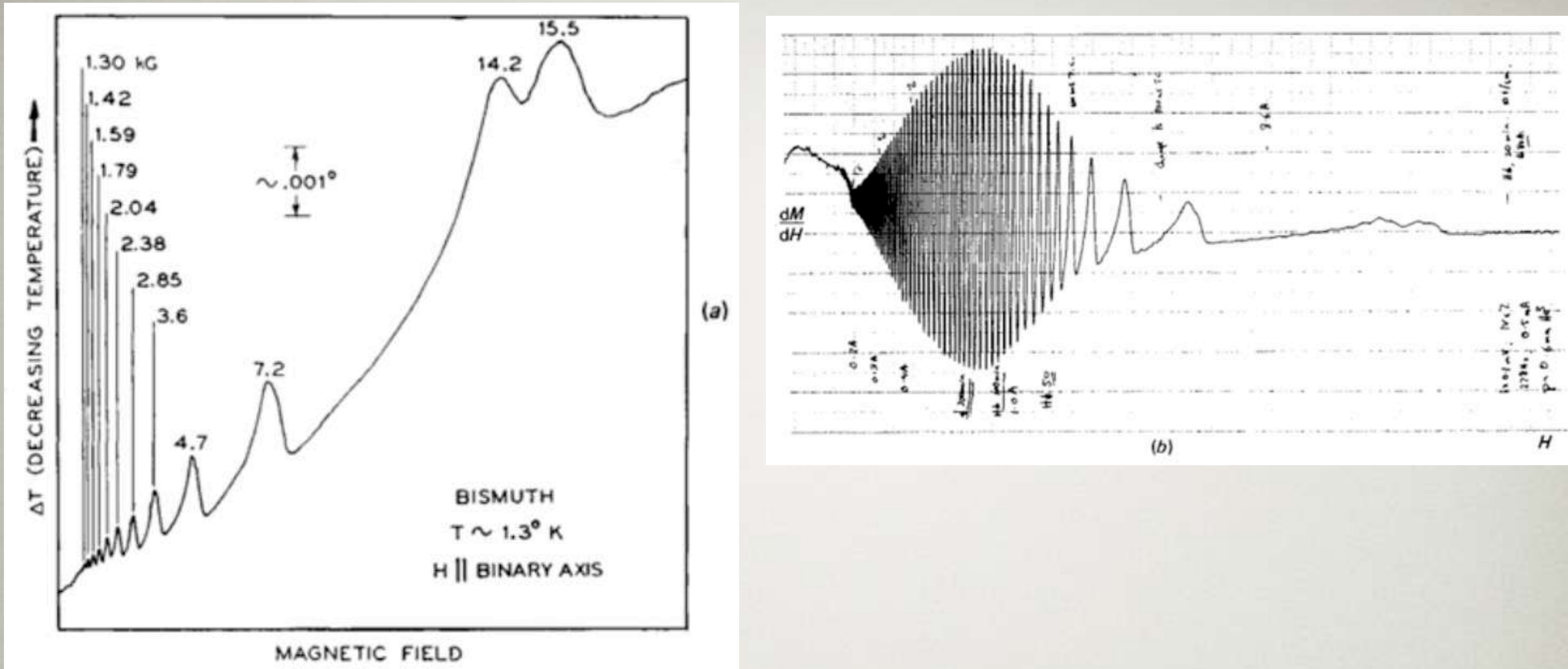

Fig. 4.1. (*a*) Magnetothermal oscillations in Bi for H along a binary axis (Kunzler *et al.* 1962) $T \sim 1.3\,\mathrm{K}$. (*b*) dHvA oscillations of $\mathrm{d}M/\mathrm{d}H$, $T \sim 0.6\,\mathrm{K}$ (unpublished data of Barklie and Shoenberg 1974). The rate of sweep was not uniform, so distance along chart is not quite linear in H; the fields of the various oscillations are as marked in (*a*). Spin-splitting in the last oscillation (and the next to last in (*b*)) is clearly visible. Comparison of (*a*) and (*b*) illustrates the similarity of line shape in the two effects and the difference of the H dependence of amplitude. However, the comparison can only be qualitative since (*a*) and (*b*) are at different temperatures on different crystals and moreover $z \ll 1$ is true for only the last two or three oscillations before the quantum limit (at about 15 kG). Further illustrations of the oscillations of $\mathrm{d}M/\mathrm{d}H$ in Bi are shown in figs. 8.8 and 8.9.

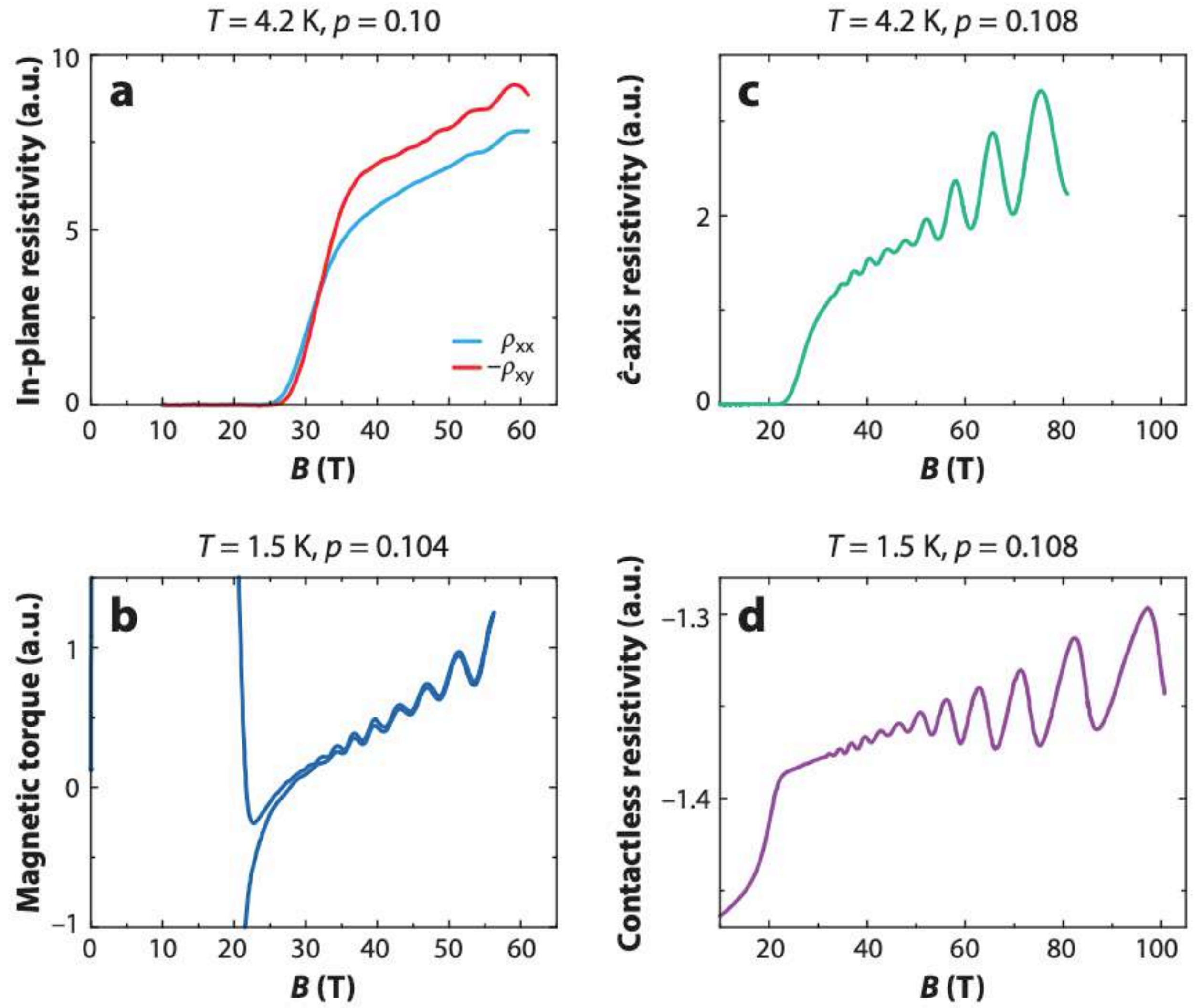

Figure 2

Quantum oscillations measured in underdoped $YBa_2Cu_3O_{6+\delta}$ by a variety of experimental techniques, including (*a*) in-plane four contact resistivity (data from 32), (*b*) magnetic torque (data from 45), (*c*) $\hat{c}$-axis four contact resistivity (data from 39), and (*d*) contactless resistivity measured using a resonant proximity detection oscillator (data from 35).

Quantum Oscillations in Hole-Doped Cuprates

Suchitra E. Sebastian[1] and Cyril Proust[2]

[1]Cavendish Laboratory, Cambridge University, Cambridge CB3 0HE, United Kingdom; email: ses59@cam.ac.uk

[2]Laboratoire National des Champs Magnétiques Intenses, UPR 3228 (CNRS-INSA-UJF-UPS), Toulouse 31400, France; email: cyril.proust@lncmi.cnrs.fr

Annual Review of Condensed Matter Physics

Vol. 6:411-430 (Volume publication date March 2015)

https://doi.org/10.1146/annurev-conmatphys-030212-184305

Vol 438|10 November 2005|doi:10.1038/nature04233 nature

LETTERS

Two-dimensional gas of massless Dirac fermions in graphene

K. S. Novoselov[1], A. K. Geim[1], S. V. Morozov[2], D. Jiang[1], M. I. Katsnelson[3], I. V. Grigorieva[1], S. V. Dubonos[2] & A. A. Firsov[2]

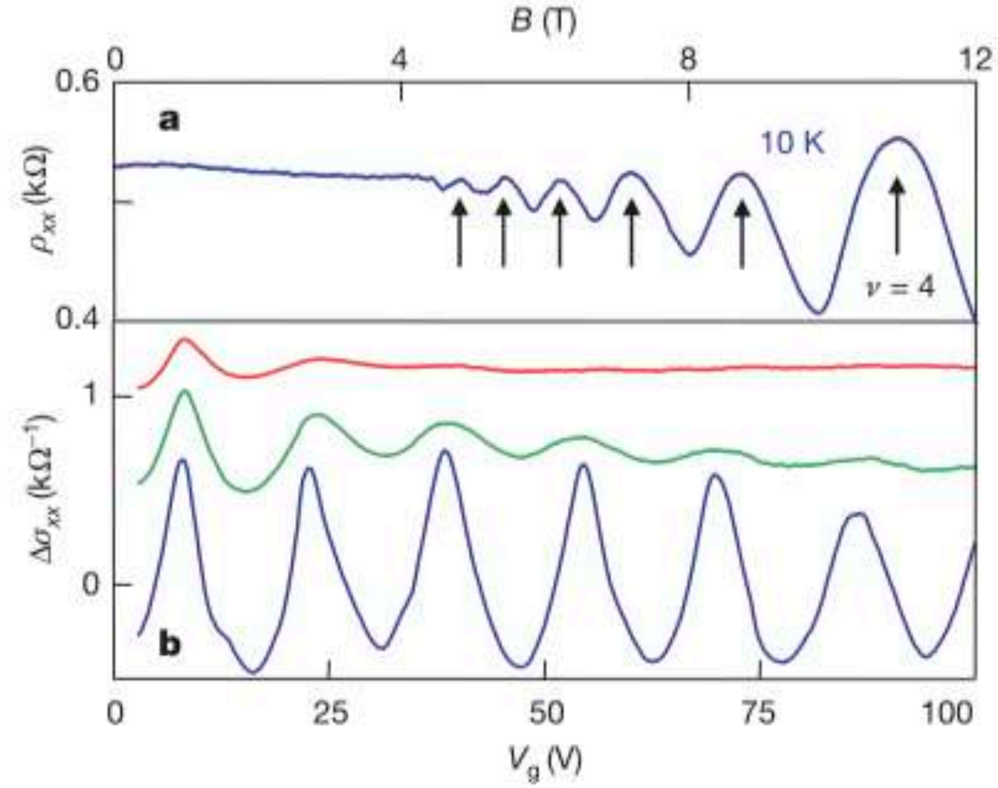

Figure 2 | Quantum oscillations in graphene. SdHO at constant gate voltage $V_g = -60$ V as a function of magnetic field B (**a**) and at constant $B = 12$ T as a function of V_g (**b**). Because μ does not change greatly with V_g, the measurements at constant B (at a constant $\omega_c\tau = \mu B$) were found more informative. In **b**, SdHOs in graphene are more sensitive to T at high carrier concentrations: blue, $T = 20$ K; green, $T = 80$ K; red, $T = 140$ K. The $\Delta\sigma_{xx}$ curves were obtained by subtracting a smooth (nearly linear) increase in σ with increasing V_g and are shifted for clarity. SdHO periodicity ΔV_g at constant B is determined by the density of states at each Landau level ($\alpha\Delta V_g = fB/\phi_0$), which for the observed periodicity of ~15.8 V at $B = 12$ T yields a quadruple degeneracy. Arrows in **a** indicate integer ν (for example, $\nu = 4$ corresponds to 10.9 T) as found from SdHO frequency $B_F \approx 43.5$ T. Note the absence of any significant contribution of universal conductance fluctuations (see also Fig. 1) and weak localization magnetoresistance, which are normally intrinsic for 2D materials with so high resistivity.

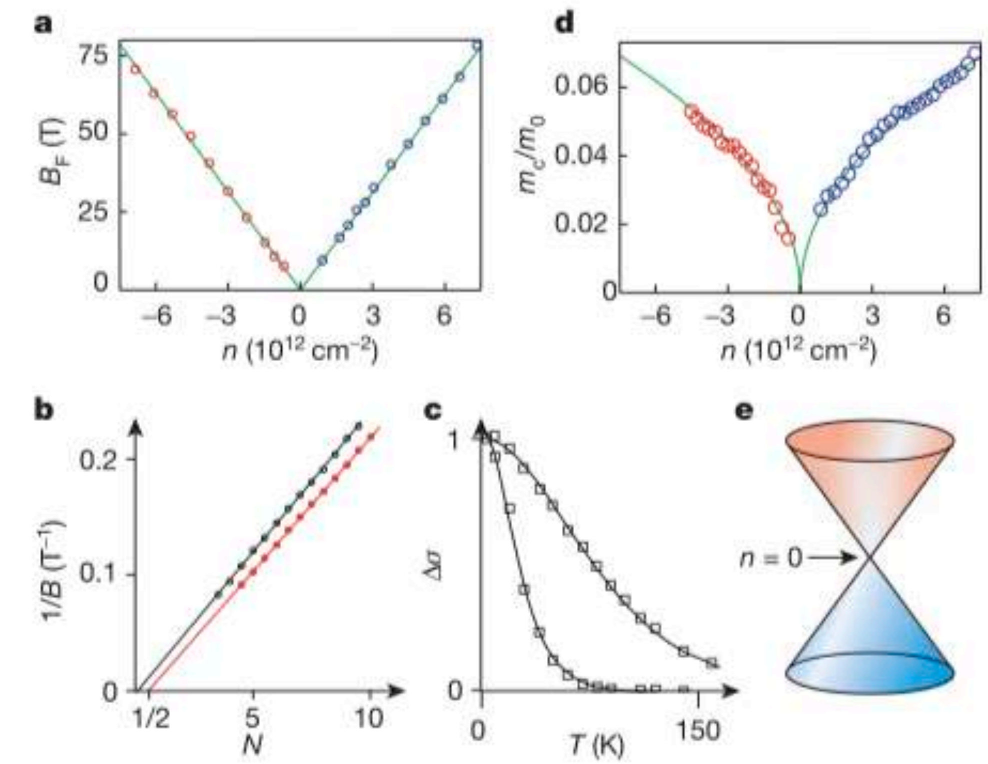

Figure 3 | Dirac fermions of graphene. **a**, Dependence of B_F on carrier concentration n (positive n corresponds to electrons; negative to holes). **b**, Examples of fan diagrams used in our analysis[7] to find B_F. N is the number associated with different minima of oscillations. The lower and upper curves are for graphene (sample of Fig. 2a) and a 5-nm-thick film of graphite with a similar value of B_F, respectively. Note that the curves extrapolate to different origins, namely to $N = 1/2$ and $N = 0$. In graphene, curves for all n extrapolate to $N = 1/2$ (compare ref. 7). This indicates a phase shift of π with respect to the conventional Landau quantization in metals. The shift is due to Berry's phase[14,20]. **c**, Examples of the behaviour of SdHO amplitude $\Delta\sigma$ (symbols) as a function of T for $m_c \approx 0.069$ and $0.023m_0$ (see the dependences showing the rapid and slower decay with increasing T, respectively); solid curves are best fits. **d**, Cyclotron mass m_c of electrons and holes as a function of their concentration. Symbols are experimental data, solid curves the best fit to theory. **e**, Electronic spectrum of graphene, as inferred experimentally and in agreement with theory. This is the spectrum of a zero-gap 2D semiconductor that describes massless Dirac fermions with c_* 1/300 the speed of light.

REPORT

GRAPHENE

High-temperature quantum oscillations caused by recurring Bloch states in graphene superlattices

R. Krishna Kumar,[1,2,3] X. Chen,[2] G. H. Auton,[2] A. Mishchenko,[1] D. A. Bandurin,[1] S. V. Morozov,[4,5] Y. Cao,[2] E. Khestanova,[1] M. Ben Shalom,[1] A. V. Kretinin,[2,6] K. S. Novoselov,[2] L. Eaves,[2,7] I. V. Grigorieva,[1] L. A. Ponomarenko,[3] V. I. Fal'ko,[1,2]* A. K. Geim[1,2]*

Cyclotron motion of charge carriers in metals and semiconductors leads to Landau quantization and magneto-oscillatory behavior in their properties. Cryogenic temperatures are usually required to observe these oscillations. We show that graphene superlattices support a different type of quantum oscillation that does not rely on Landau quantization. The oscillations are extremely robust and persist well above room temperature in magnetic fields of only a few tesla. We attribute this phenomenon to repetitive changes in the electronic structure of superlattices such that charge carriers experience effectively no magnetic field at simple fractions of the flux quantum per superlattice unit cell. Our work hints at unexplored physics in Hofstadter butterfly systems at high temperatures.

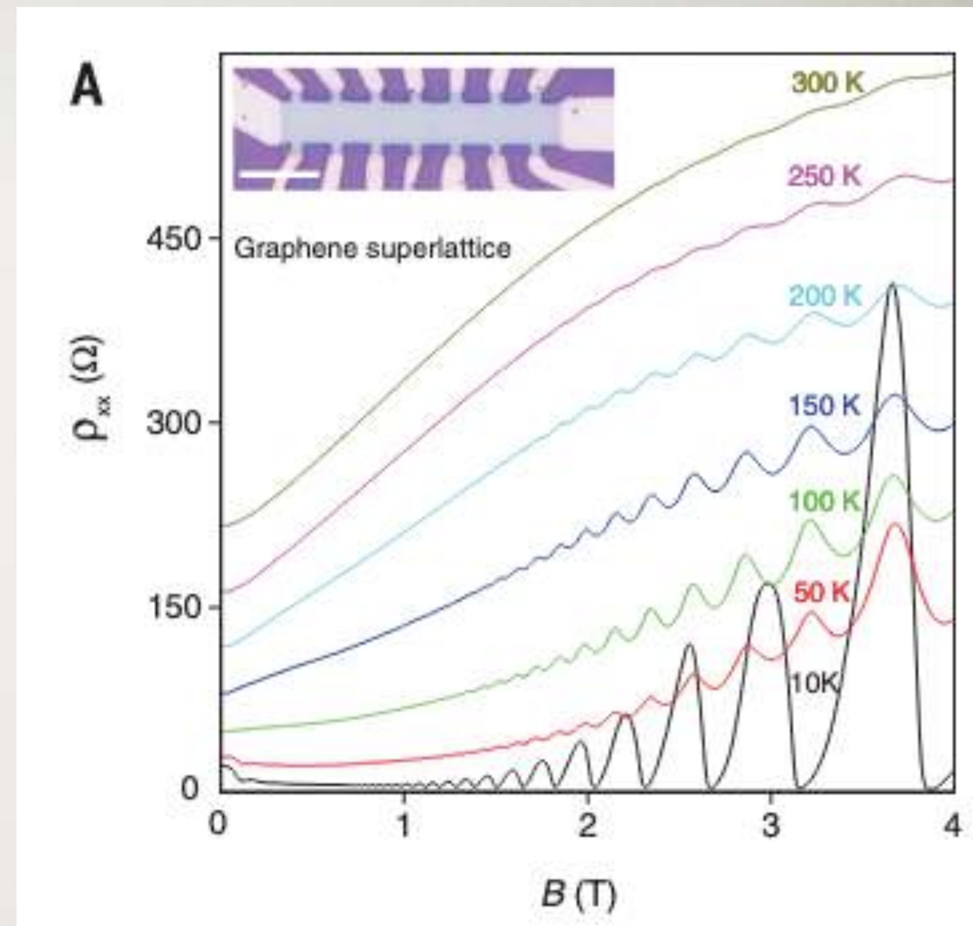

Krishna Kumar *et al.*, *Science* **357**, 181–184 (2017)   14 July 2017

$$F = \Phi_0 \, n_\sigma$$ SdH

$$F = \Phi_0 \, \frac{p}{q}$$ BZ = Brown-Zak

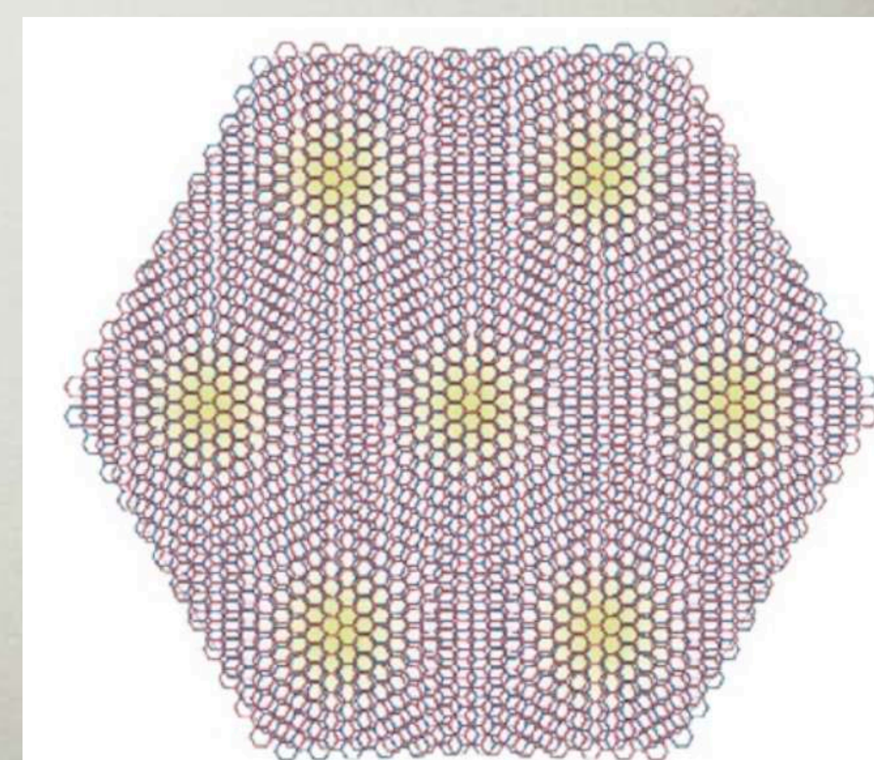

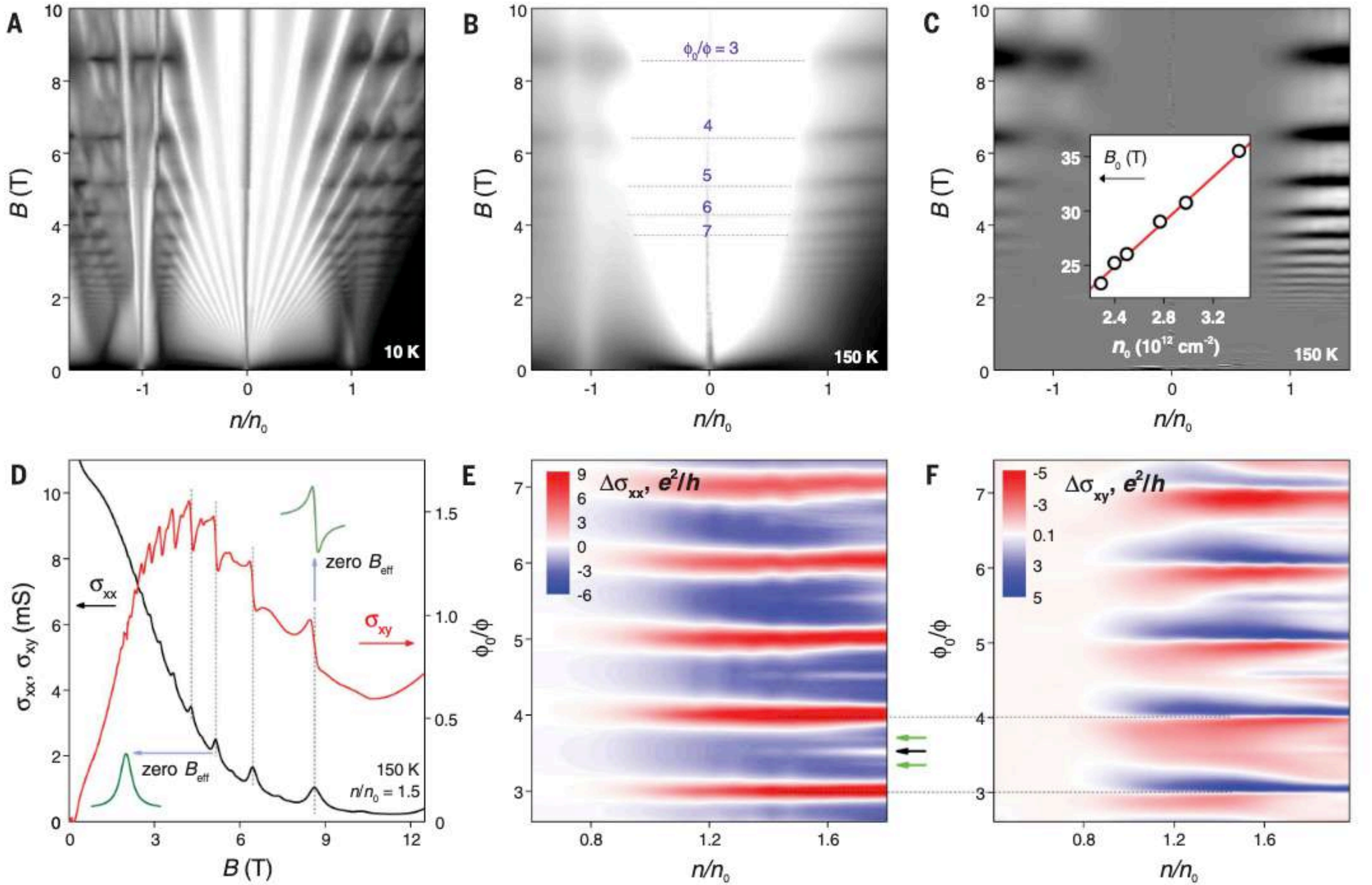

Fig. 2. Concentration and field dependence of Brown-Zak (BZ) oscillations. (**A**) Low-T fan diagram $\sigma_{xx}(n, B)$ for a superlattice device with $a \approx$ 13.9 nm. The gray scale is logarithmic: white, 0.015 mS; black, 15 mS. (**B**) Same device as (A) but at 150 K. Logarithmic gray scale: white, 0.1 mS; black, 10 mS. The dotted lines denote $B = \phi_0/qS$. (**C**) Same as (B) but for $\Delta\sigma_{xx}$ obtained by subtracting a smooth best-fit background (26). Linear gray scale: ±0.3 mS. (Inset) Fundamental frequency B_0 of BZ oscillations found in our different devices as a function of $n_0 = 8/\sqrt{3}a^2$. (**D**) Near $B = \phi_0/qS$ (dashed lines are for q = 3 to 6), local changes in σ_{xx} and σ_{xy} resemble magnetotransport in metals near zero field, as illustrated by the green inset curves. (**E**) Part of (C) near the second-generation NP for electron doping is magnified and plotted as a function of ϕ_0/ϕ. The main maxima in $\Delta\sigma_{xx}$ occur at $\phi_0/\phi = q$. A few extra maxima for p = 2 and 3 are indicated by black and green arrows, respectively (see fig. S6 for details). (**F**) Corresponding behavior of $\Delta\sigma_{xy}$ (smooth background subtracted). Its zeros align with the red maxima in $\Delta\sigma_{xx}$.

PHYSICAL REVIEW VOLUME 133, NUMBER 4A 17 FEBRUARY 1964

Bloch Electrons in a Uniform Magnetic Field*

E. BROWN
Rensselaer Polytechnic Institute, Troy, New York
(Received 29 August 1963)

The physical periodicity of a space lattice is not destroyed by the presence of a uniform magnetic field. It is shown that a ray group of unitary operators, isomorphic to pure translations, commutes with the Hamiltonian in this case. Such a group has the characteristic property that $AB=\exp[i\phi(A,B)]C$, where A, B, and C are elements of the group and ϕ is a numerical factor. Representation theory applied to this group yields the characteristic degeneracies of levels in magnetic fields, as well as the transformation properties of eigenfunctions. By means of these it is possible to construct an effective Hamiltonian appropriate to finite magnetic fields in crystals.

PHYSICAL REVIEW VOLUME 134, NUMBER 6A 15 JUNE 1964

Magnetic Translation Group*

J. ZAK
National Magnet Laboratory,† Massachusetts Institute of Technology, Cambridge, Massachusetts
(Received 6 December 1963)

In this paper a group-theoretical approach to the problem of a Bloch electron in a magnetic field is given. A magnetic translation group is defined and its properties, in particular its connection with the usual translation group, are established.

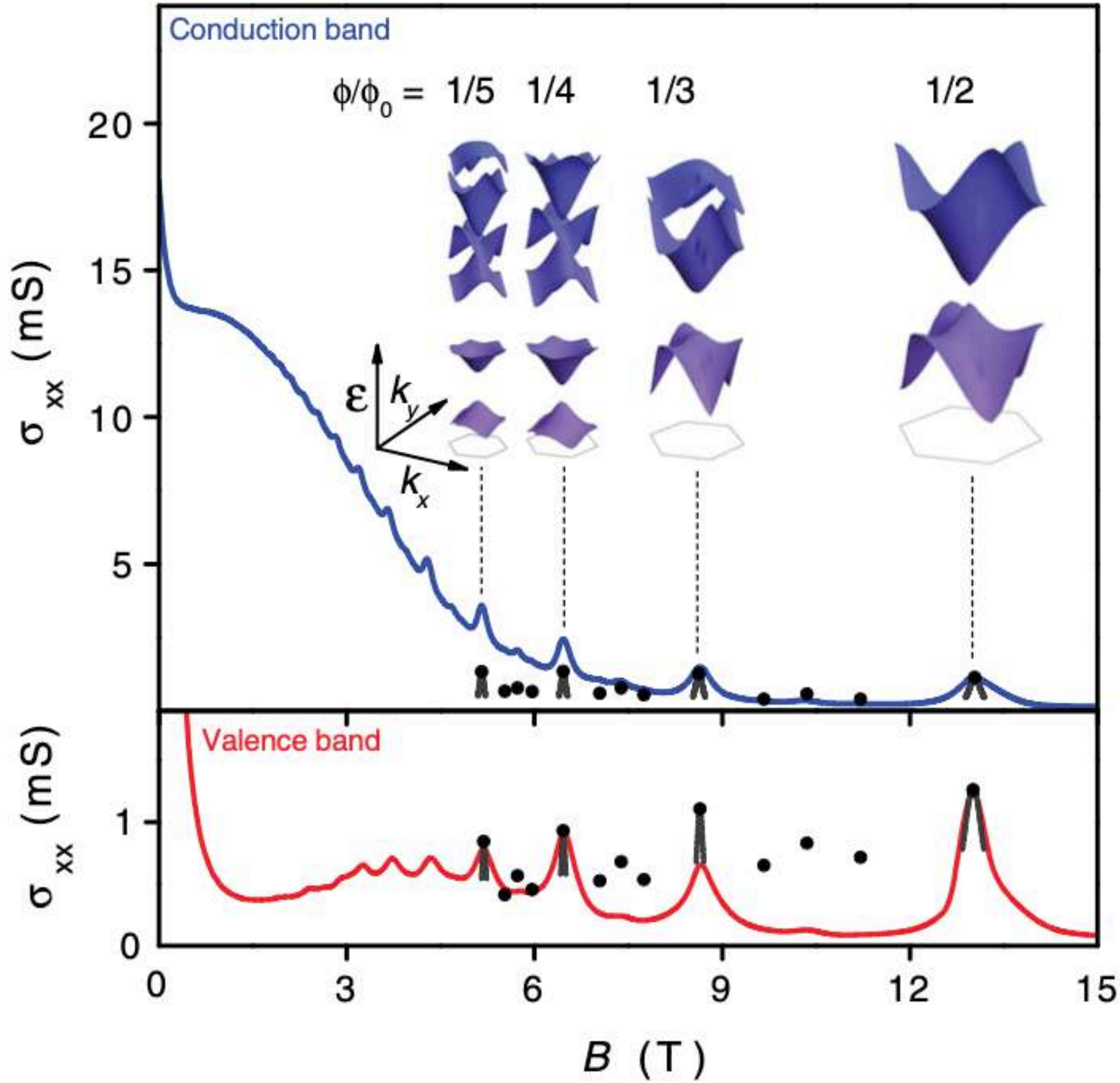

Fig. 3. BZ oscillations as recurring Bloch states in small effective fields. Solid curves: σ_{xx} at 100 K for electron and hole doping ($n/n_0 = \pm1.6$) (top and bottom panels, respectively) in a superlattice device with $a \approx$ 13.6 nm. Black dots and curves: σ_{xx} calculated in the constant-τ approximation for different p and q. Inset image: BZ minibands $\varepsilon(\vec{\mathbf{k}})$ inside the first Brillouin zones indicated by the gray hexagons (their size decreases with increasing q). The minibands were calculated for a generic graphene-on-hBN superlattice (*29*) and correspond to broadened LLs (for example, LLs are 2 and 3 for q = 2 and range from 3 to 8 for q = 5). Only those minibands at energies relevant to the doping level on the experimental curves are shown.

High-order fractal states in graphene superlattices

R. Krishna Kumar[a,b], A. Mishchenko[a,b], X. Chen[b], S. Pezzini[c], G. H. Auton[b], L. A. Ponomarenko[d], U. Zeitler[c], L. Eaves[a,e], V. I. Fal'ko[a,b,1], and A. K. Geim[a,b,1]

[a]School of Physics & Astronomy, University of Manchester, M13 9PL Manchester, United Kingdom; [b]National Graphene Institute, University of Manchester, M13 9PL Manchester, United Kingdom; [c]High Field Magnet Laboratory, Radboud University, 6525 ED Nijmegen, The Netherlands; [d]Department of Physics, University of Lancaster, LA1 4YW Lancaster, United Kingdom; and [e]School of Physics and Astronomy, University of Nottingham, NG7 2RD Nottingham, United Kingdom

Contributed by A. K. Geim, April 11, 2018 (sent for review March 16, 2018; reviewed by Allan H. MacDonald and Barbaros Oezyilmaz)

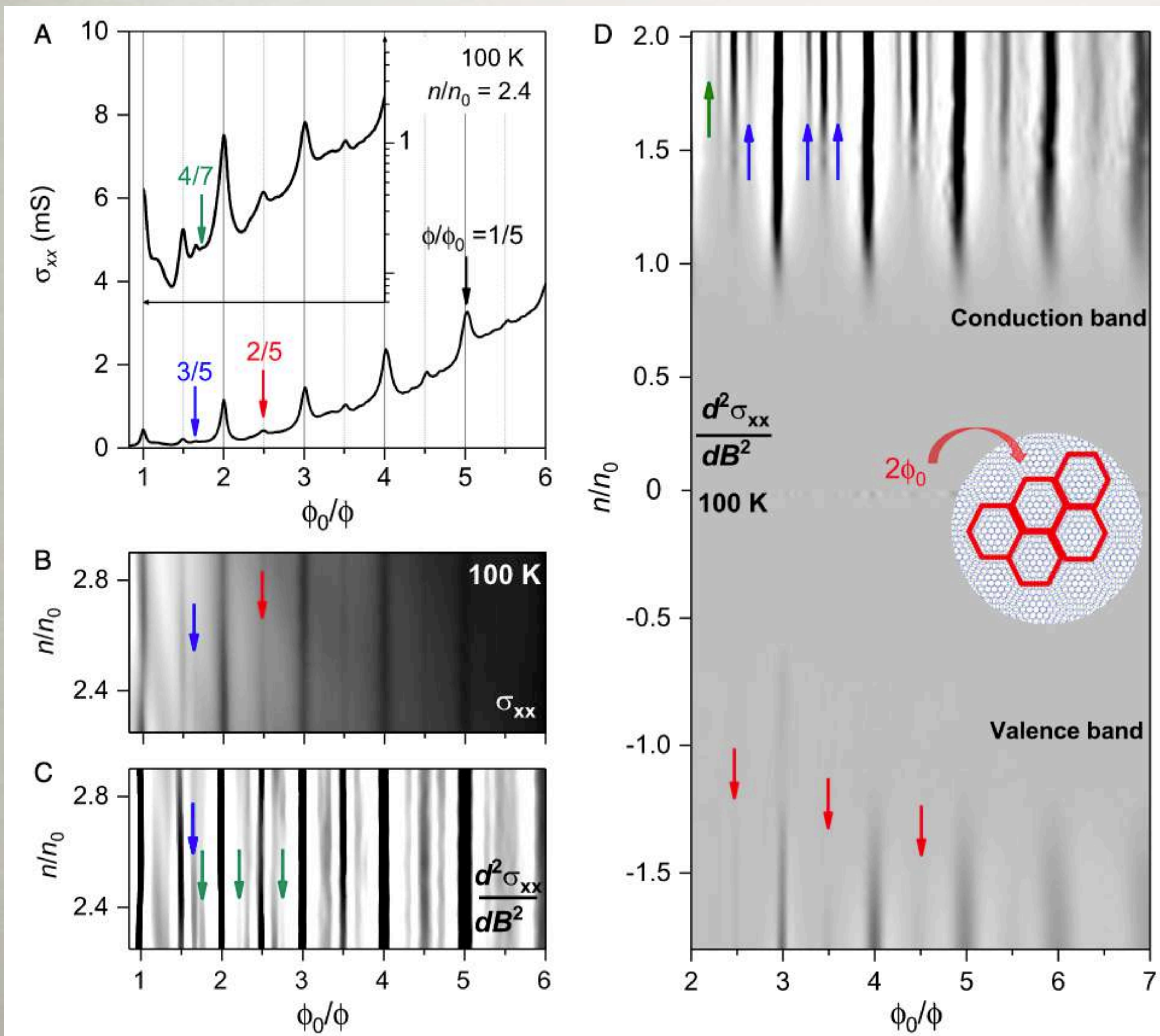

$$F = \Phi_0 \, \frac{p}{q}$$

$$p > 1$$

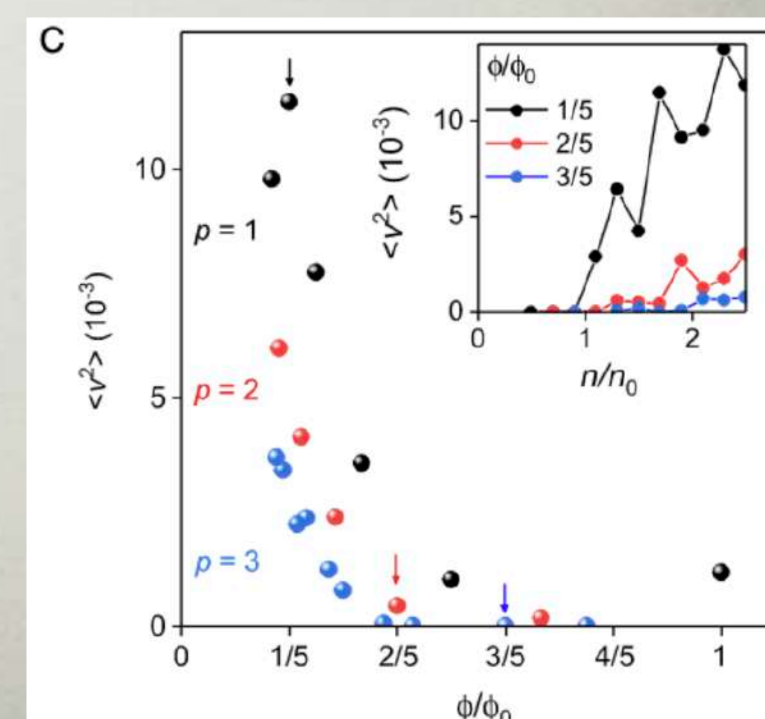

ARTICLE

https://doi.org/10.1038/s41467-020-19604-0 OPEN

Long-range ballistic transport of Brown-Zak fermions in graphene superlattices

Julien Barrier[1,2,5], Piranavan Kumaravadivel[1,2,5], Roshan Krishna Kumar[1,2], L. A. Ponomarenko[1,3], Na Xin[1,2], Matthew Holwill[2], Ciaran Mullan[1], Minsoo Kim[1], R. V. Gorbachev[1,2], M. D. Thompson[3], J. R. Prance[3], T. Taniguchi[4], K. Watanabe[4], I. V. Grigorieva[1,2], K. S. Novoselov[1,2], A. Mishchenko[1,2], V. I. Fal'ko[1,2], A. K. Geim[1,2✉] & A. I. Berdyugin[1,2✉]

In quantizing magnetic fields, graphene superlattices exhibit a complex fractal spectrum often referred to as the Hofstadter butterfly. It can be viewed as a collection of Landau levels that arise from quantization of Brown-Zak minibands recurring at rational (p/q) fractions of the magnetic flux quantum per superlattice unit cell. Here we show that, in graphene-on-boron-nitride superlattices, Brown-Zak fermions can exhibit mobilities above 10^6 cm^2 V^{-1} s^{-1} and the mean free path exceeding several micrometers. The exceptional quality of our devices allows us to show that Brown-Zak minibands are $4q$ times degenerate and all the degeneracies (spin, valley and mini-valley) can be lifted by exchange interactions below 1 K. We also found negative bend resistance at $1/q$ fractions for electrical probes placed as far as several micrometers apart. The latter observation highlights the fact that Brown-Zak fermions are Bloch quasiparticles propagating in high fields along straight trajectories, just like electrons in zero field.

bend resistance

$$R_b = \frac{V_b}{I}$$

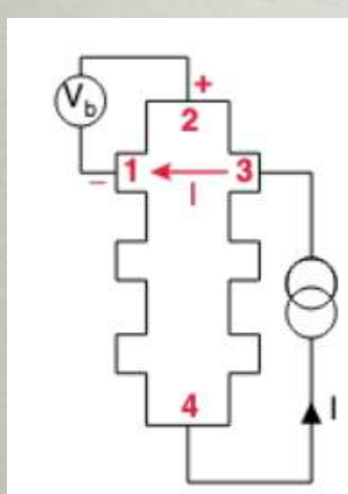

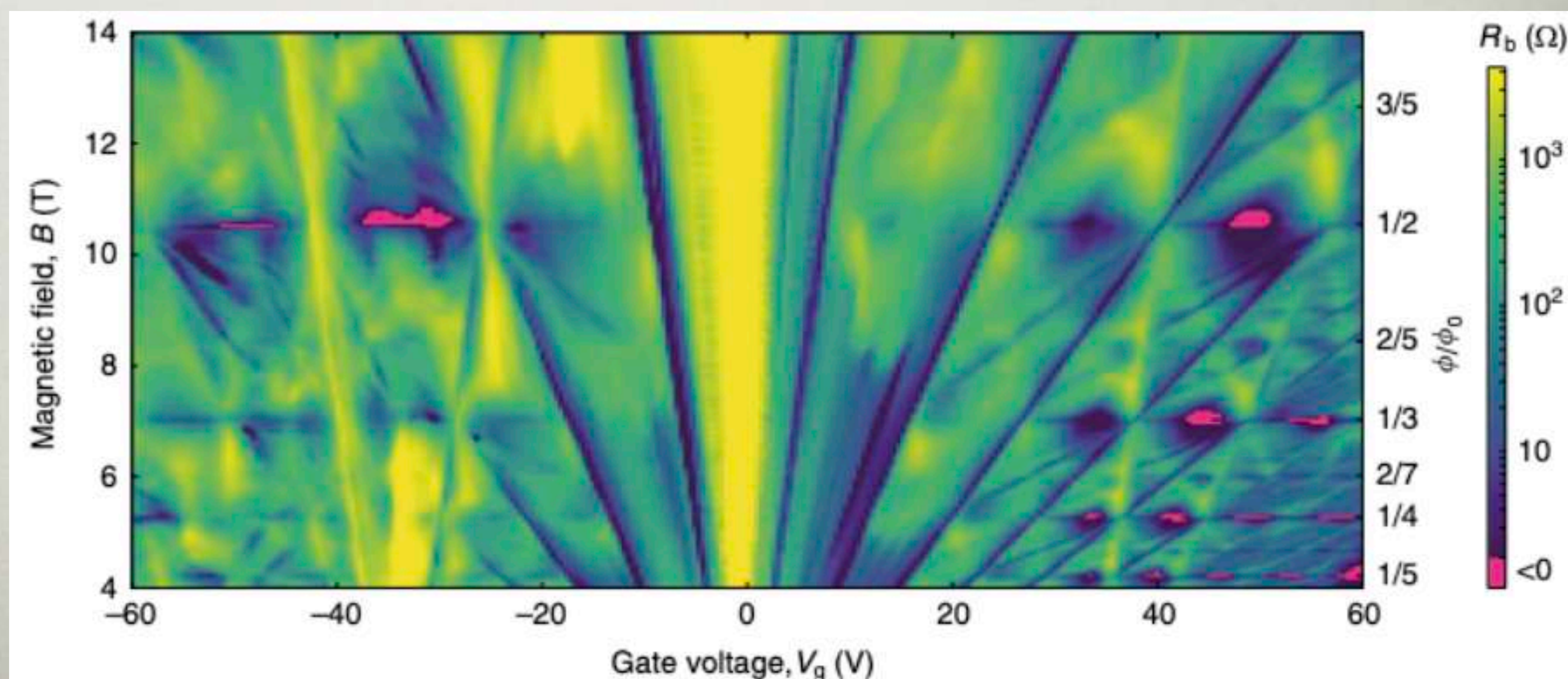

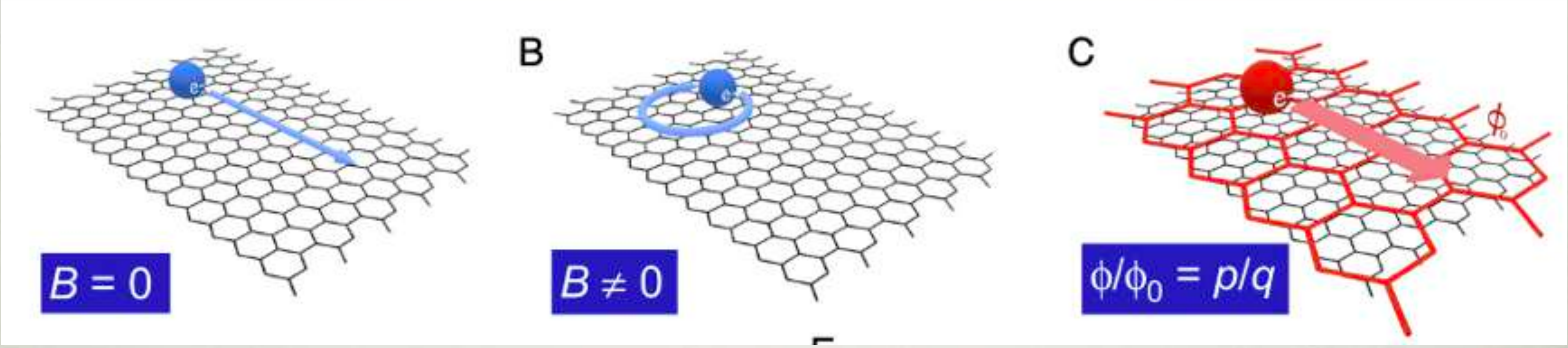

Is this the most appropriate picture?

[1] J. Vučičević and R. Žitko, "Universal magnetic oscillations of dc conductivity in the incoherent regime of correlated systems," Phys. Rev. Lett. **127**, 196601 (2021).
[2] J. Vučičević and R. Žitko, "Electrical conductivity in the Hubbard model: Orbital effects of magnetic field," Phys. Rev. B **104**, 205101 (2021).

1. Establish formalism for computing σ^{xx} and σ^{xy} for Hubbard model on 2D square lattice using the DMFT at arbitrary temperature T, magnetic field B, and electron density n
2. Generalization and real-space formulation of the "Khurana argument": absence of vertex corrections (in DMFT) for σ^{xx} and σ^{xy}
3. Comprehensive data for σ in all regimes
4. Observation of SdH and BZ oscillations
5. Explain BZ oscillations as non-elastic processes which change the magnetic quantum number:

BZ oscillations are "activated by incoherence"

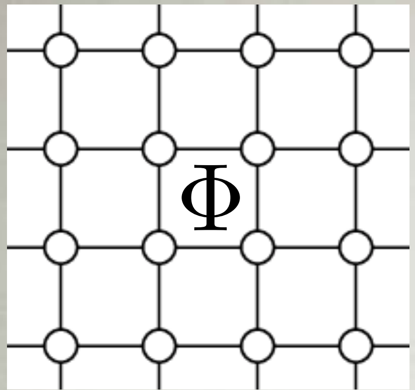

$$\Phi = B_z a^2$$

flux per plaquette

$$H_0 = -\mu \sum_{i,\sigma} n_{i,\sigma} + g\mu_B \sum_i \mathbf{B}(\mathbf{r}_i) \cdot \mathbf{S}_i - \sum_{i,j,\sigma} t_{ij} e^{if_{ij}} c^\dagger_{i,\sigma} c_{j,\sigma}$$

Hubbard model

$$H_{\rm int} = U \sum_i n_{i,\uparrow} n_{i,\downarrow}$$

$$S_i^\eta = \frac{1}{2}(c^\dagger_{i,\uparrow},\ c^\dagger_{i,\downarrow})\hat{\sigma}^\eta \begin{pmatrix} c_{i,\uparrow} \\ c_{i,\downarrow} \end{pmatrix}$$

$$f_{ij} = \frac{e}{\hbar} \int_{\mathbf{r}_i}^{\mathbf{r}_j} \mathbf{A}(\mathbf{r}) \cdot d\mathbf{r}$$

Peierls phase

$$\mathbf{A}(\mathbf{r}) = (0, xB_z, 0)$$

Landau gauge

$$\begin{aligned} f_{ij} &\equiv f_{\mathbf{r}_i,\mathbf{r}_j} \\ &= \frac{e}{\hbar}(B_z a^2)\frac{(y_j - y_i)(x_i + x_j)}{2} \\ &= 2\pi \frac{\Phi}{\Phi_0} \frac{(y_j - y_i)(x_i + x_j)}{2}, \end{aligned}$$

$$\Phi_0 = h/e$$

unit flux

periodic magnetic cells for rational p/q flux

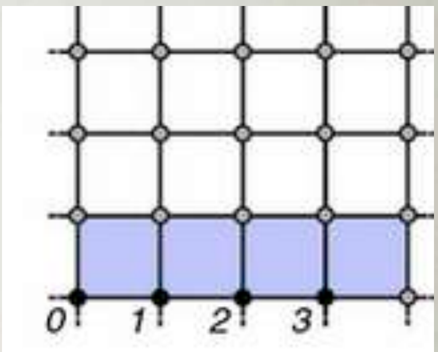

q=4

$$\frac{e}{\hbar}(B_z a^2) = 2\pi \frac{p}{q} = 2\pi \frac{n}{L}$$

$$\begin{aligned} H_{\text{kin}} &= -t \sum_{i,\mathbf{u}\in\{\mathbf{e}_x,\mathbf{e}_y\},\sigma} e^{i2\pi \frac{n}{L} x_i \mathbf{u}\cdot\mathbf{e}_y} c^\dagger_{\mathbf{r}_i,\sigma} c_{\mathbf{r}_i+\mathbf{u},\sigma} + \text{H.c.} \\ &= -2t \sum_{\mathbf{k},\sigma} \cos k_x n_{\mathbf{k},\sigma} - t \sum_{\mathbf{k},\sigma} e^{ik_y} c^\dagger_{\mathbf{k},\sigma} c_{\mathbf{k}-2\pi \frac{n}{L}\mathbf{e}_x,\sigma} + \text{H.c.} \end{aligned}$$

$\tilde{k}_x \in [0, 2\pi/q)$ $\quad c_{\tilde{\mathbf{k}},l,\sigma} \equiv c_{\mathbf{k}=\tilde{\mathbf{k}}+l\frac{2\pi}{q}\mathbf{e}_x,\sigma}$ $\quad l \in [0, q)$

(l: quantum number associated with the q sites of the magnetic unit cell)

eigenvectors contain detailed information about the orbital effects of the field on electrons

$$c^\dagger_{\tilde{\mathbf{k}},l,\sigma} = \sum_m [\alpha_{\tilde{\mathbf{k}},\sigma}]_{l,m} c^\dagger_{\tilde{\mathbf{k}},m,\sigma}$$

eigenbasis (m: seniority)

$$\bar{G}_{ij,\sigma}(z) \equiv e^{-if_{ij}} G_{ij,\sigma}(z)$$

Gauge invariant Green's function:
preserves the full symmetry of the lattice

$$\bar{\boldsymbol{\Sigma}}(z) \equiv \boldsymbol{\Sigma}(z) \circ e^{-i\bar{\mathbf{f}}}$$

(In PRB we give perturbative proof for the case of local density-density interactions.)

DMFT (dynamical mean-field theory) approximation: Σ is local.
Using gauge invariant objects, the DMFT construction proceeds without modification!

$$\mathbf{G}(z) = [\mathbf{I}\hbar z - \mathbf{H}_0[\mathbf{A}] - \mathbf{I}\Sigma^{\mathrm{imp}}(z)]^{-1}$$

$$\Sigma_{\sigma,ij} = \delta_{ij}\Sigma_\sigma \Longrightarrow \langle \tilde{\mathbf{k}}, \sigma, m|\boldsymbol{\Sigma}|\tilde{\mathbf{k}}', \sigma, m'\rangle = \delta_{\tilde{\mathbf{k}},\tilde{\mathbf{k}}'}\delta_{m,m'}\Sigma_\sigma$$

$$G_{\tilde{\mathbf{k}},m,m',\sigma}(z) = \delta_{mm'} G_{\tilde{\mathbf{k}},mm,\sigma}(z)$$

DOS including the Peierls-phase effects

$$G_{ii,\sigma}(z) = \int d\varepsilon \frac{\rho_0(\varepsilon)}{\hbar z - \varepsilon - \Sigma_\sigma(z)}$$

Acheche, Arsenault, Trembley, PRB (2017)

$$\mathbf{E} = \partial_t \mathbf{A}^{\text{ext}}$$

the vector potential due to electrical field is a small long-wavelength correction to the vector potential due to magnetic field

$$-\int \mathbf{j}(\mathbf{r}) \cdot \mathbf{A}^{\text{ext}}(\mathbf{r}) d^3\mathbf{r} = -v_{\text{cell}} \sum_i \mathbf{j}_{\mathbf{r}_i} \cdot \mathbf{A}^{\text{ext}}_{\mathbf{r}_i}$$

$$v_{\text{cell}} = a^2 c$$

$$\frac{e}{\hbar} \int_{a\mathbf{r}_i}^{a\mathbf{r}_j} \mathbf{A}^{\text{ext}}(\mathbf{r}) \cdot d\mathbf{r} \approx \frac{ea}{\hbar} \mathbf{A}^{\text{ext}} \cdot (\mathbf{r}_j - \mathbf{r}_i)$$

$$H_{\text{kin}} = -t \sum_{i,\mathbf{u} \in \{\mathbf{e}_x, \mathbf{e}_y\}, \sigma} e^{i\left(f_{\mathbf{r}_i, \mathbf{r}_i+\mathbf{u}} + \frac{ea}{\hbar} \mathbf{A}^{\text{ext}}_{\mathbf{r}_i} \cdot \mathbf{u}\right)} c^\dagger_{\mathbf{r}_i,\sigma} c_{\mathbf{r}_i+\mathbf{u},\sigma} + \text{H.c.}$$

$$\begin{aligned} \mathbf{j}_{\mathbf{r}} &= -\frac{1}{v_{\text{cell}}} \frac{\partial H}{\partial \mathbf{A}^{\text{ext}}_{\mathbf{r}}} \bigg|_{\mathbf{A}^{\text{ext}} \to 0} \\ &= it \frac{1}{ac} \frac{e}{\hbar} \sum_{\mathbf{u} \in \{\mathbf{e}_x, \mathbf{e}_y\}, \sigma} \mathbf{u} e^{i f_{\mathbf{r}_i, \mathbf{r}_i+\mathbf{u}}} c^\dagger_{\mathbf{r}_i,\sigma} c_{\mathbf{r}_i+\mathbf{u},\sigma} + \text{H.c.} \end{aligned}$$

$$\begin{aligned} \Lambda^{\eta\eta'}_{\mathbf{r},\mathbf{r}'}(\tau) &= \langle j^\eta_{\mathbf{r}}(\tau) j^{\eta'}_{\mathbf{r}'}(0) \rangle - \langle j^\eta_{\mathbf{r}} \rangle \langle j^{\eta'}_{\mathbf{r}'} \rangle \\ &= -t^2 \frac{1}{a^2 c^2} \frac{e^2}{\hbar^2} \sum_{\sigma,\sigma'} \sum_{b,b' \in \{0,1\}} (-1)^{b+b'} C^b[\gamma_\eta(\mathbf{r})] C^{b'}[\gamma_{\eta'}(\mathbf{r}')] \\ &\quad \times \langle c^\dagger_{\mathbf{r}+b\mathbf{e}_\eta,\sigma}(\tau^+) c_{\mathbf{r}+(1-b)\mathbf{e}_\eta,\sigma}(\tau) c^\dagger_{\mathbf{r}'+b'\mathbf{e}_{\eta'},\sigma'}(0^+) c_{\mathbf{r}'+(1-b')\mathbf{e}_{\eta'},\sigma'}(0) \rangle - \langle j^\eta_{\mathbf{r}} \rangle \langle j^{\eta'}_{\mathbf{r}'} \rangle \end{aligned}$$

linear-response (Kubo) theory

$$\Lambda^{\eta\eta'}_{\mathbf{q}=0}(\tau) = v_{\text{cell}} \sum_{\mathbf{r}} \Lambda_{\mathbf{r},\mathbf{r}'=0}(\tau)$$

$$\Lambda^{\eta\eta'}_{\mathbf{q}=0}(i\nu) = v_{\text{cell}} \sum_{\mathbf{r}} \frac{1}{2\hbar} \int_{-\beta\hbar}^{\beta\hbar} d\tau\, e^{i\nu\tau} \Lambda_{\mathbf{r},\mathbf{r}'=0}(\tau)$$

$$\Lambda^{\eta\eta'}_{\mathbf{q}=0}(i\nu) = \frac{V}{2\hbar} \int_{-\beta\hbar}^{\beta\hbar} d\tau \langle j^{\eta}_{\mathbf{q}=0}(\tau) j^{\eta'}_{\mathbf{q}=0}(0)\rangle \qquad V = N v_{\text{cell}}$$

$$j^{\eta}_{\mathbf{q}=0} = \frac{1}{N} \sum_{\mathbf{r}} j^{\eta}_{\mathbf{r}}$$

$$j^{\eta}_{\mathbf{q}=0} = \frac{it}{N} \frac{1}{ac} \frac{e}{\hbar} \sum_{\sigma} \sum_{\tilde{\mathbf{k}},m,m'} v^{\eta}_{\tilde{\mathbf{k}},m,m',\sigma} c^{\dagger}_{\tilde{\mathbf{k}},m,\sigma} c_{\tilde{\mathbf{k}},m',\sigma}$$

velocity vertexes

$$v^{x}_{\tilde{\mathbf{k}},m,m',\sigma} = \sum_{l} [\alpha_{\tilde{\mathbf{k}},\sigma}]_{l,m} [\alpha_{\tilde{\mathbf{k}},\sigma}]^{*}_{l,m'} \left[e^{i\tilde{k}_x} e^{il\frac{2\pi}{q}} - e^{-i\tilde{k}_x} e^{-il\frac{2\pi}{q}} \right]$$

$$v^{y}_{\tilde{\mathbf{k}},m,m',\sigma} = \sum_{l} [\alpha_{\tilde{\mathbf{k}},\sigma}]_{l,m} \left[e^{i\tilde{k}_y} [\alpha_{\tilde{\mathbf{k}},\sigma}]^{*}_{l\ominus p,m'} - e^{-i\tilde{k}_y} [\alpha_{\tilde{\mathbf{k}},\sigma}]^{*}_{l\oplus p,m'} \right]$$

diagonal in $\tilde{k}$, but matrix-valued in "m space"

$$\Lambda^{\eta\eta',\mathrm{disc}}_{\mathbf{q}=\mathbf{0}}(i\nu) = \frac{t^2 e^2}{c\hbar^2}\frac{1}{N}\sum_{\sigma}\sum_{\tilde{\mathbf{k}},m_1,m_1',m_2,m_2'} \times v^{\eta}_{\tilde{\mathbf{k}},m_1,m_1',\sigma} v^{\eta'}_{\tilde{\mathbf{k}},m_2,m_2',\sigma} \times \frac{1}{\beta}\sum_{i\omega} G_{\tilde{\mathbf{k}},m_2',m_1\sigma}(i\omega) G_{\tilde{\mathbf{k}},m_1',m_2,\sigma}(i\omega + i\nu)$$

bubble contribution

$$G_{\tilde{\mathbf{k}},m,m',\sigma}(z) = \delta_{mm'} G_{\tilde{\mathbf{k}},mm,\sigma}(z)$$

DMFT case

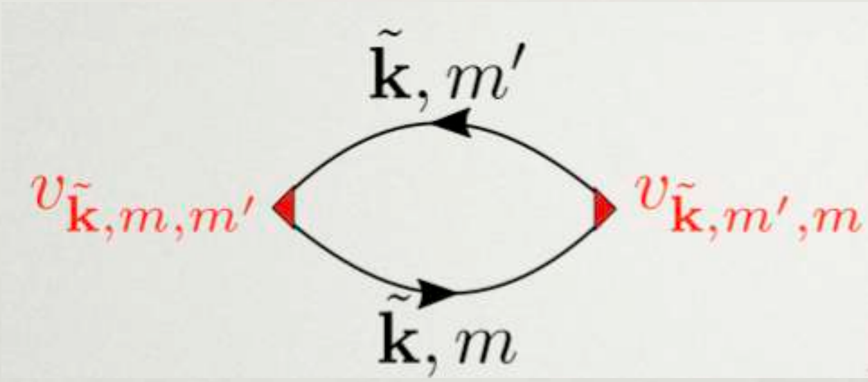

$$v^{\eta,\eta'}_{\sigma}(\varepsilon, \varepsilon') \equiv \frac{1}{N}\sum_{\tilde{\mathbf{k}},m,m'} \delta(\varepsilon - \varepsilon_{\tilde{\mathbf{k}},m,\sigma}) \times \delta(\varepsilon' - \varepsilon_{\tilde{\mathbf{k}},m',\sigma}) v^{\eta}_{\tilde{\mathbf{k}},m,m',\sigma} v^{\eta'}_{\tilde{\mathbf{k}},m',m,\sigma}$$

velocity kernel

The *sheet conductance* is related to the current-current correlation function through

$$\sigma^{\eta\eta'}(\nu) = c\frac{\Lambda^{\eta\eta'}(\nu) - \Lambda^{\eta\eta'}(\nu = 0)}{i\,\nu}. \qquad (69)$$

The z-axis lattice constant c cancels out c from $v_{\mathrm{cell}} = a^2 c$ and its value is irrelevant. In the following we will discard the difference between the sheet conductance and the conductivity, and refer to σ as conductivity, even though it is actually sheet conductance and the units of the two quantities are different [$(\Omega m)^{-1}$ vs Ω^{-1}, respectively]; this is common practice in the field.

$$\mathrm{Re}\sigma^{xx,\mathrm{disc}}_{\mathbf{q}=\mathbf{0}}(\nu = 0) = t^2\frac{e^2}{\hbar}\frac{1}{\pi}\sum_\sigma \int d\varepsilon \int d\varepsilon' v^{xx}_\sigma(\varepsilon,\varepsilon')\int d\omega \times \mathrm{Im}G(\varepsilon,\ \omega)\mathrm{Im}G(\varepsilon',\ \omega)n'_{\mathrm{F}}(\omega), \qquad (70)$$

longitudinal conductivity

$$n'_{\mathrm{F}}(\omega) = -\beta\hbar e^{\beta\hbar\omega}/(1 + e^{\beta\hbar\omega})^2$$

$$\mathrm{Re}\sigma^{xy,\mathrm{disc}}_{\mathbf{q}=\mathbf{0}}(\nu = 0) = -t^2\frac{e^2}{\hbar}\frac{1}{\pi^2}\sum_\sigma \int d\varepsilon \int d\varepsilon' \mathrm{Im}v^{xy}_\sigma(\varepsilon,\varepsilon')\int d\omega \int d\omega' \times \mathrm{Im}G(\varepsilon,\ \omega)\mathrm{Im}G(\varepsilon',\ \omega')\frac{n_{\mathrm{F}}(\omega) - n_{\mathrm{F}}(\omega')}{(\omega - \omega')^2}. \qquad (71)$$

Hall conductivity

See also Markov, Rohringer, Rubtsov, PRB 2019

Vertex correction cancellation for any gauge choice, for all components of j-j tensor

$$
\begin{aligned}
&\Lambda^{\eta\eta',\mathrm{conn}}_{\mathbf{q}=0}(\tau-\tau') \\
&= t^2 \frac{e^2}{a^2c^2\hbar^2}\sum_{\sigma,\sigma'}\sum_{b,b'\in\{0,1\}}(-1)^{b+b'} \\
&\quad\times \frac{1}{N^2}\sum_{\mathbf{r},\mathbf{r}'} C^b[\gamma_\eta(\mathbf{r})]C^{b'}[\gamma_{\eta'}(\mathbf{r}')] \\
&\quad\times \sum_{\mathbf{r}_1,\mathbf{r}_2,\mathbf{r}_3,\mathbf{r}_4}\int d\tau_1 d\tau_2 d\tau_3 d\tau_4 \\
&\quad\times G_{\mathbf{r}_1,\mathbf{r}+b\mathbf{e}_\eta,\sigma}(\tau_1-\tau)G_{\mathbf{r}+(1-b)\mathbf{e}_\eta,\mathbf{r}_2,\sigma}(\tau-\tau_2) \\
&\quad\times F((\mathbf{r}_1,\tau_1),(\mathbf{r}_2,\tau_2),(\mathbf{r}_3,\tau_3),(\mathbf{r}_4,\tau_4)) \\
&\quad\times G_{\mathbf{r}'+(1-b')\mathbf{e}_{\eta'},\mathbf{r}_3,\sigma'}(\tau'-\tau_3)G_{\mathbf{r}_4,\mathbf{r}'+b'\mathbf{e}_{\eta'},\sigma'}(\tau_4-\tau')
\end{aligned}
$$

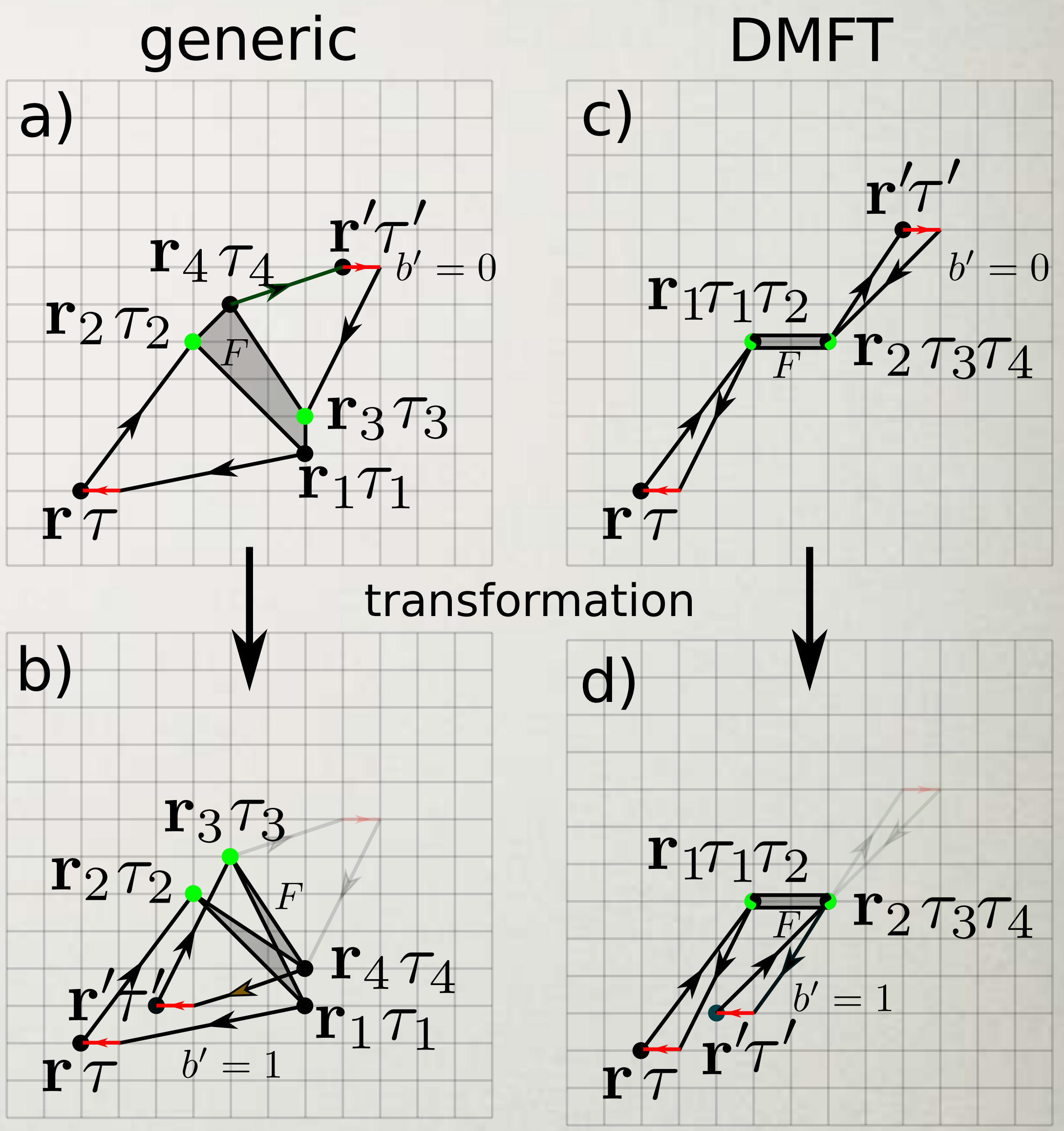

$$
\mathbf{r}' \to -\mathbf{r}' + \mathbf{r}_3 + \mathbf{r}_4 - \mathbf{e}_{\eta'}, \quad b' \to 1-b',
$$
$$
(\mathbf{r}_3,\tau_3) \leftrightarrow (\mathbf{r}_4,\tau_4).
$$

real-space version of Khurana argument

See also Markov, Rohringer, Rubtsov, PRB 2019

At low temperature we recover the conventional results:
SdH oscillations with an amplitude that
decays with increasing T according to
the standard Lifshitz-Kosevich theory.

I. M. Lifshitz and A. M. Kosevich, Zh. Éksp. Teor. Fiz. **29**, 730 (1956); [Sov. Phys. JETP **2**, 636 (1956)].
D. Schoenberg, *Magnetic Oscillations in Metals* (Cambridge University Press, Cambridge, England, 1984).

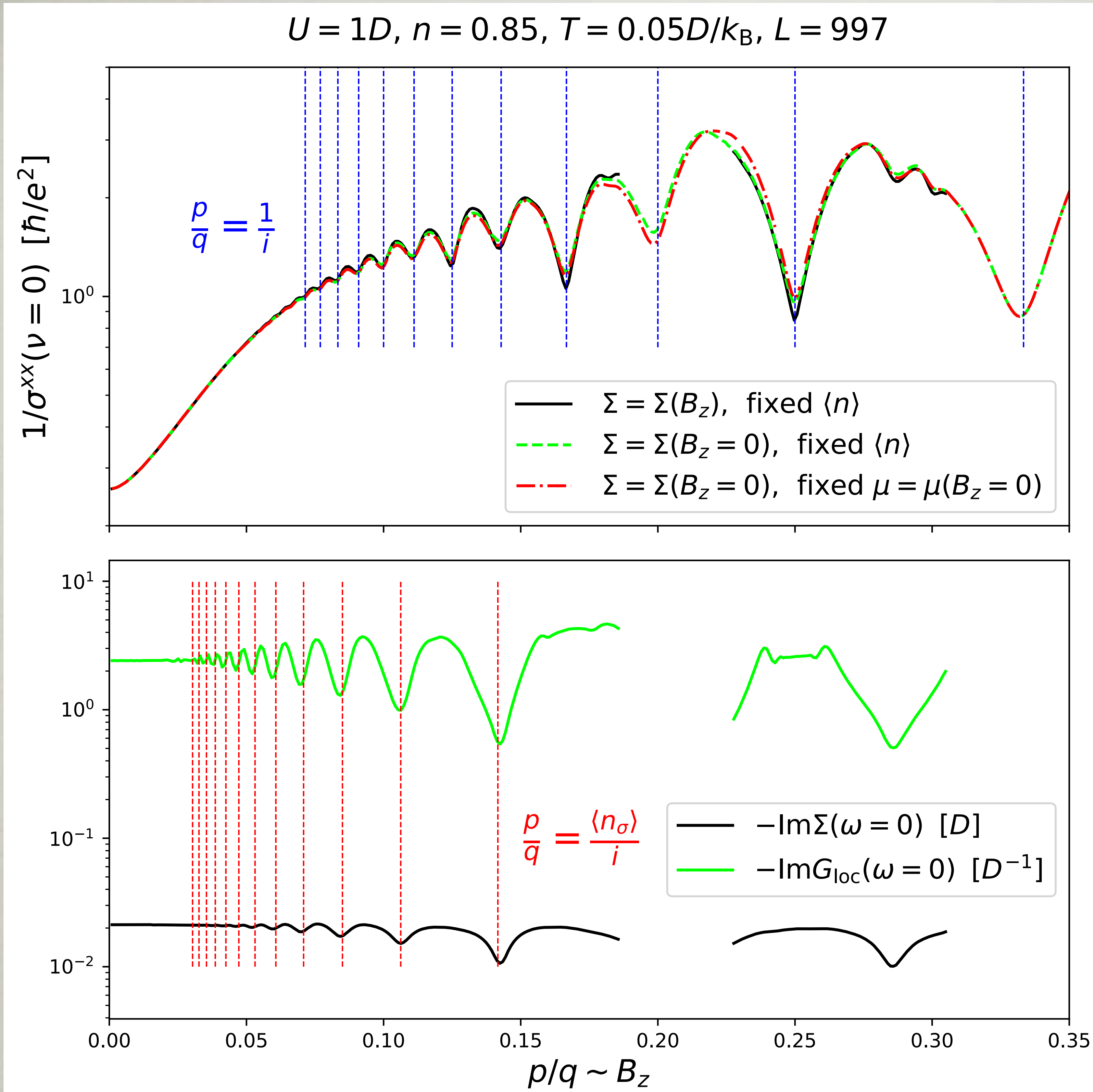

universal frequency:
depends only on unit cell size

doping-dependent
frequency

High-T: oscillations in conductivity have different frequency that those in the spectral function and scattering time!

At high enough T, it is a good approximation to use the B=0 self-energy to calculate the transport properties.
Oscillations not due to details in Σ, but due to the B-dependence of the velocity vertex!

low-T high-T

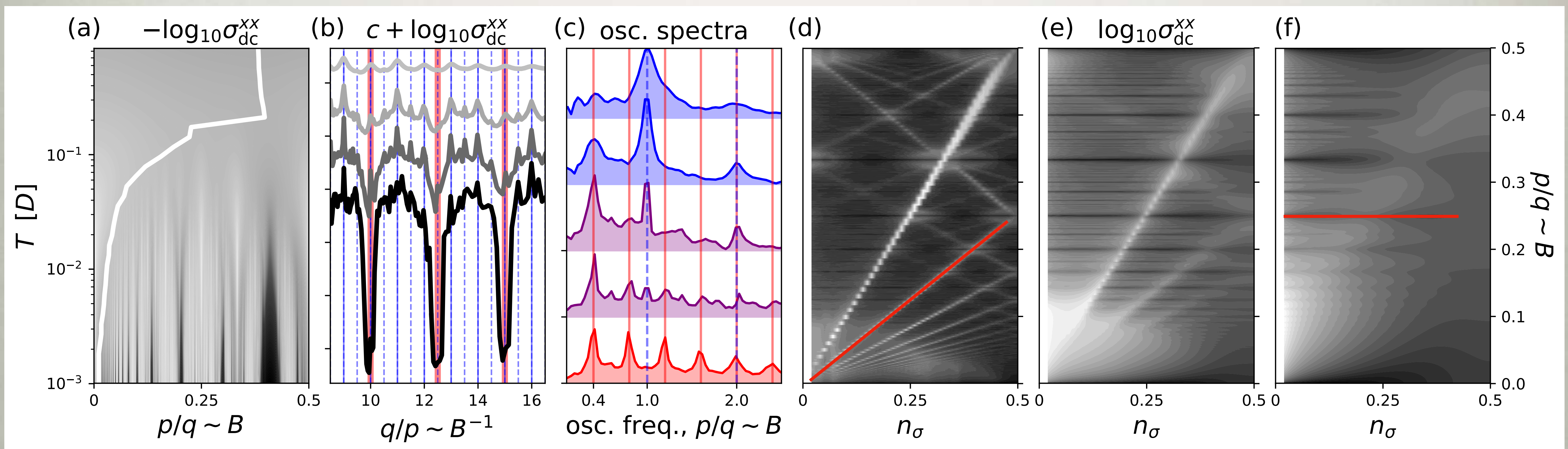

$F \propto n$ $F = \text{const.}$

Crossover: SdH oscillations at low T, coexistence, BZ oscillations at high T.

$n = 0.8, U = 1D$

finite-lifetime approximation

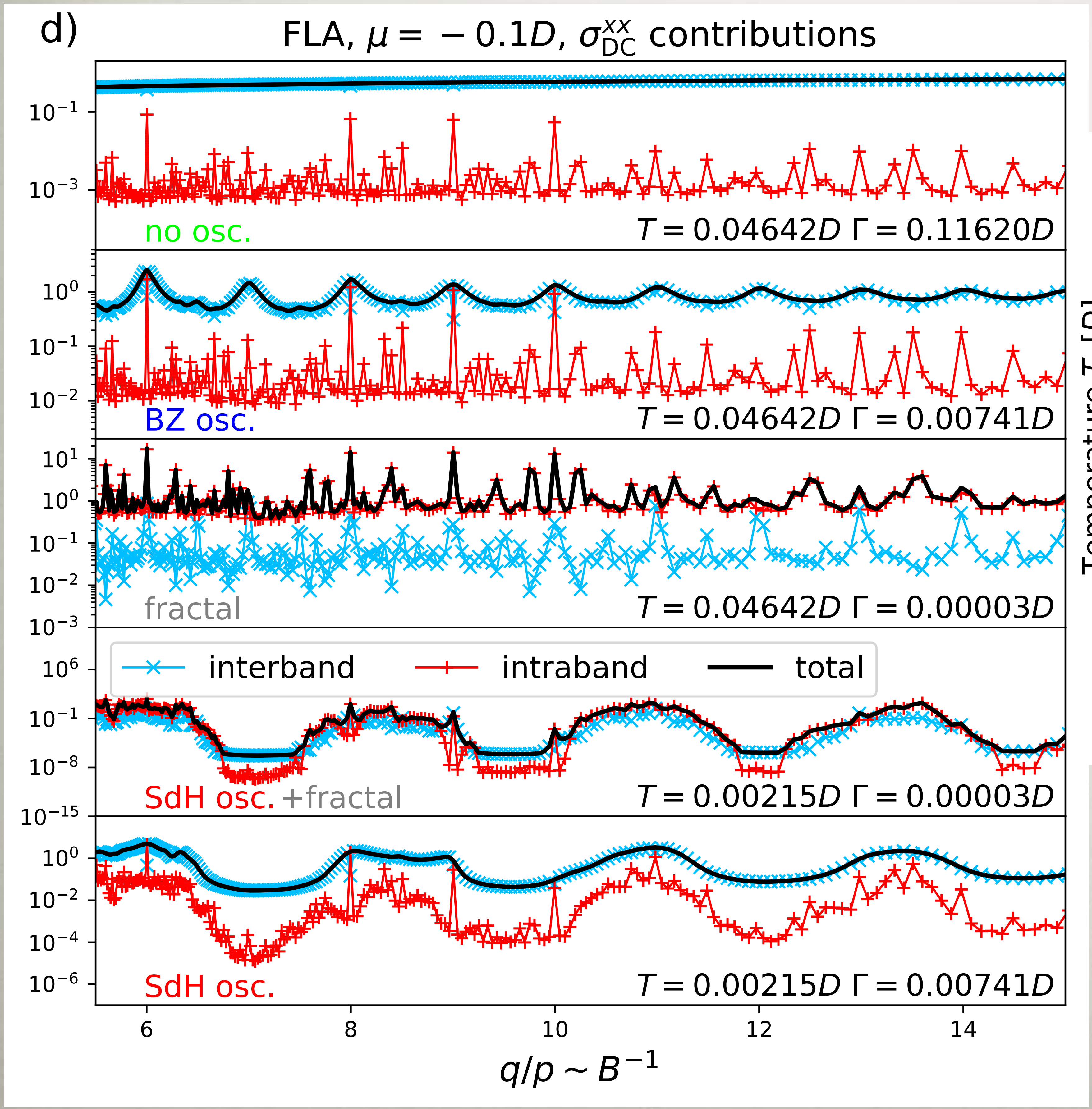

$$\Sigma_{\rm FLA}(\omega) = -i\Gamma$$

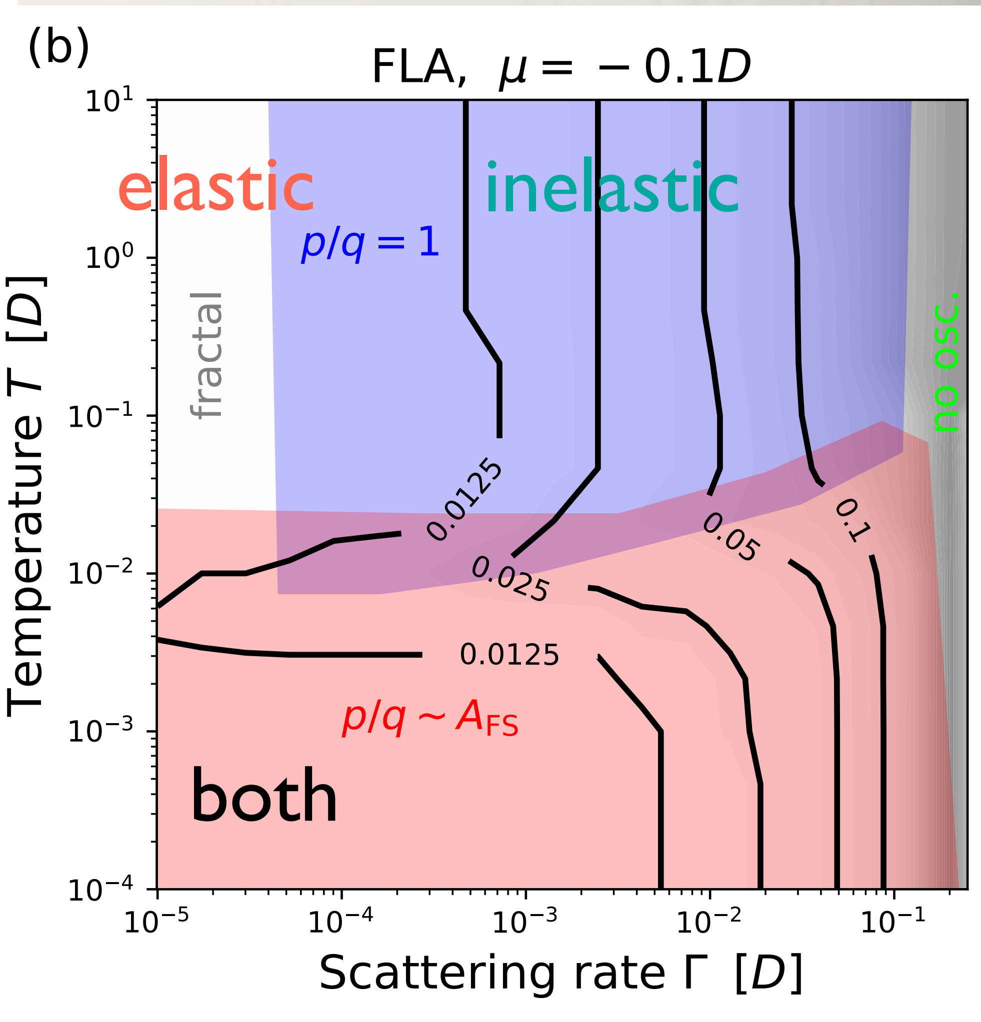

oscillation regimes in FLA

interband ~ inelastic

intraband ~ elastic

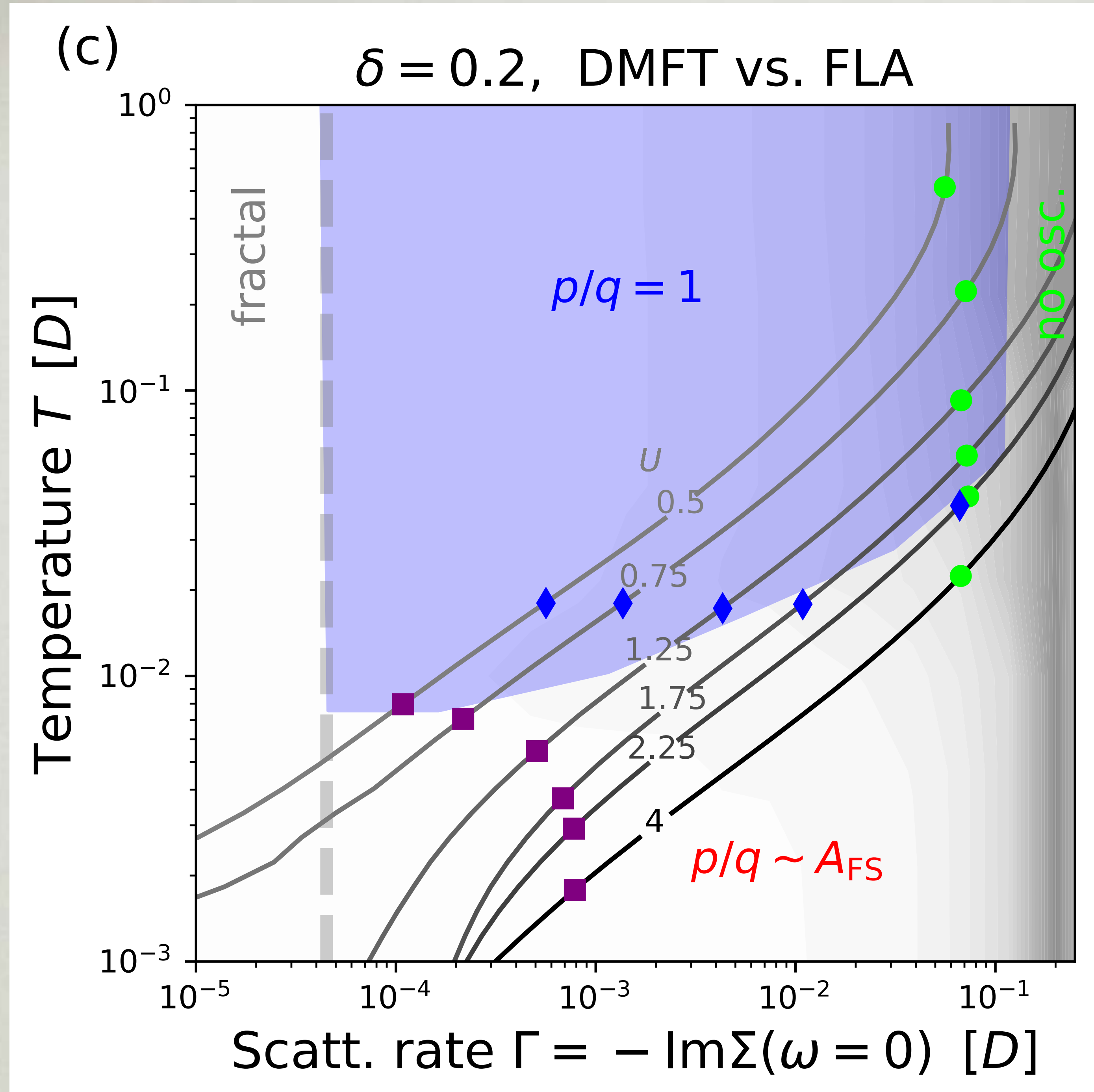

DMFT results:

high-T boundary for all oscillations

BZ dominant

BZ low-T boundary

diamonds). At low U, the lower cutoff T for BZ oscillations is also in agreement with FLA. However, at high U, the discrepancy from FLA is significant: the sinusoidal BZ oscillations appear at much lower T than one would expect based on a simple FLA toy model where Σ has no frequency dependence. At very strong U, there rather seems to be a well-defined lower cutoff Γ for regular BZ QOs extending to very low T (this lower Γ cutoff being a bit higher than the one at high T). The observation of BZ oscillations at very low T is therefore a clear indication of strong electronic correlations that go beyond simple incoherence effects.

Conclusion

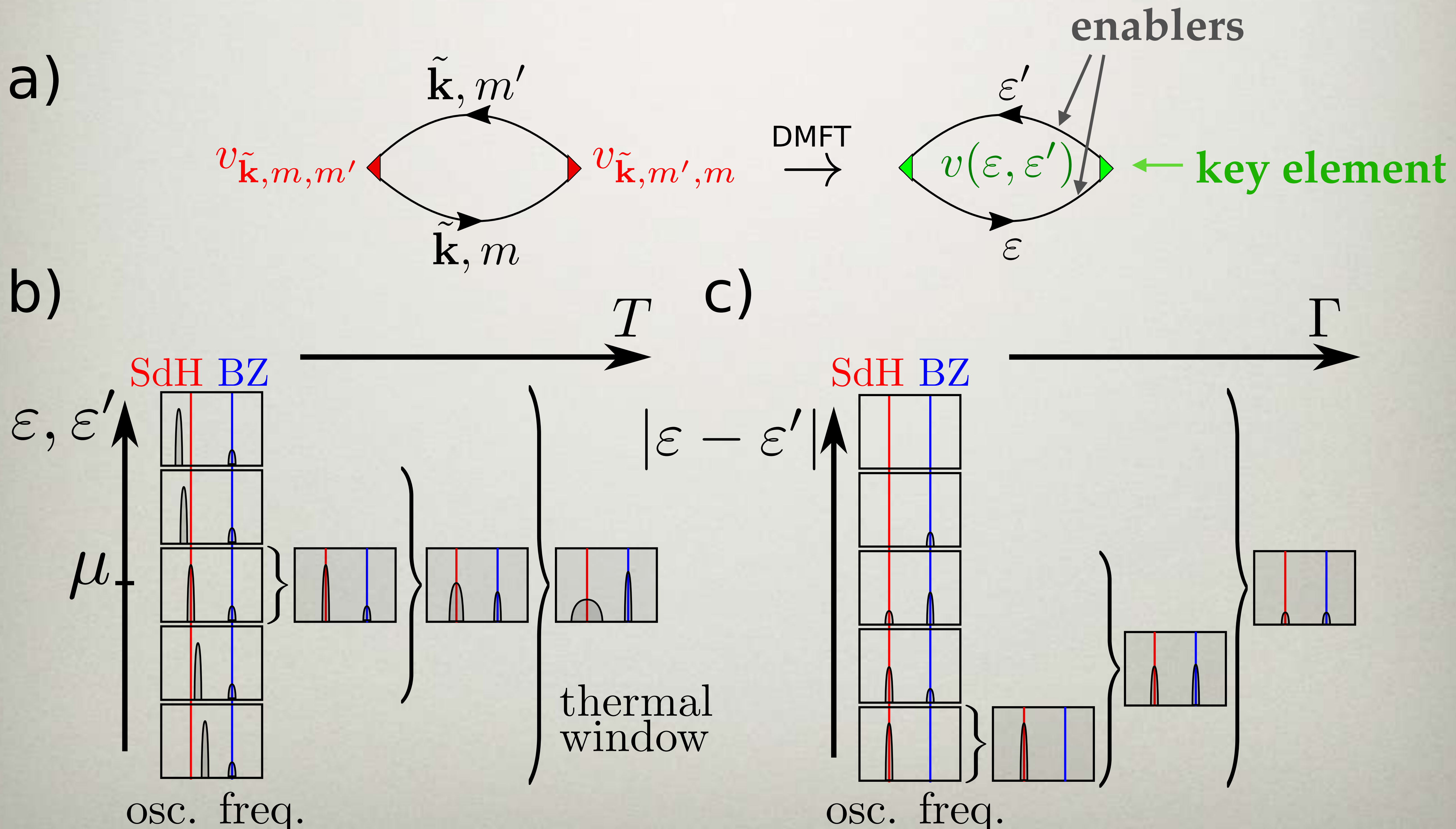
a)
$\tilde{\mathbf{k}}, m'$
$v_{\tilde{\mathbf{k}},m,m'}$
$v_{\tilde{\mathbf{k}},m',m}$
$\tilde{\mathbf{k}}, m$
DMFT
ε'
$v(\varepsilon,\varepsilon')$
ε
enablers
key element
b)
T
SdH BZ
ε,ε'
μ
thermal window
osc. freq.
c)
Γ
SdH BZ
$|\varepsilon-\varepsilon'|$
osc. freq.